Journal of Alloys and Compounds 507 (2010) 513–516

Contents lists available at ScienceDirect

Journal of Alloys and Compounds

journal homepage: www.elsevier.com/locate/jallcom

First principles study of the responses to equibiaxial in-plane tensile stresses in tetragonal $BaTiO_3$

Yifeng Duan*, Gang Tang, Lixia Qin, Liwei Shi

Department of Physics, China University of Mining and Technology, Xuzhou 221116, People's Republic of China

ARTICLE INFO

Article history:
Received 20 April 2010
Received in revised form 30 July 2010
Accepted 4 August 2010
Available online 12 August 2010

Keywords:
Phase transition
Piezoelectricity
Polarization
Epitaxial stress
Elasticity
First principles

ABSTRACT

Tetragonal $BaTiO_3$ under equibiaxial in-plane tensile stresses is investigated from first principles calculations. Our results show that this material transfers to the paraelectric phase at the critical stress of about 13 GPa. We also find the great enhancement of piezoelectricity close to the phase-transition region, due to large atomic displacements induced by stress. We also show that under the loading of applied stress, this material becomes markedly hard along the polar axis, especially at the phase-transition stress, but becomes soft along the nonpolar axes.

1. Introduction

Ferroelectrics which can convert mechanical to electrical energy (and vice versa) have wide applications in medical imaging, telecommunication and ultrasonic devices, the physical properties of which are sensitive to external conditions, such as strain, film thickness, temperature, electric and magnetic fields [1]. A new generation of single-crystal materials with high electromechanical coupling and dielectric loss properties, such as $Pb(Zn_{1/3}Nb_{2/3})$–$PbTiO_3$ (PZN-PT) and $Pb(Mg_{1/3}Nb_{2/3})O_3$–$PbTiO_3$ (PMN-PT), may further revolutionize these applications [2–4]. As one of the most common ferroelectric compounds, $BaTiO_3$, the structure of which is similar to that of single-crystal PZN-PT and PMN-PT, is a simpler system and can be taken as a model material.

The focus of this work is on the effects of equibiaxial in-plane tensile stresses on tetragonal $BaTiO_3$. The doping effects on the phase structures, magnetic and dielectric properties of $BaTiO_3$ have been systematically studied [5–7]. It is well-known that the structure and piezoelectric properties of ferroelectrics can be altered by applying external stresses (such as hydrostatic pressure) or inducing internal strains (through lattice mismatch strains in thin films) [8–10]. In fact, "strain engineering" in ferroelectrics has been widely employed to obtain desired physical and piezoelectric properties. For example, $PbTiO_3$ undergoes a complicated pressure-induced phase transitions, providing the required path for polarization rotation and eventually resulting in the giant piezoelectric responses [11]. In addition, we have revealed that the appropriate uniaxial tensile and equibiaxial compressive stresses can greatly enhance the piezoelectric strain coefficients [12,13]. Interatomic distances and the relative positions of atoms have a strong influence on the electric polarization in ferroelectric compounds. This makes it possible to control and tune polarization and piezoelectricity through in-plane misfit strains, and the corresponding biaxial stress is adjusted by the lattice mismatch between an epitaxial ferroelectric film and the underlying substrate. So far, no theoretical work has been done to study the effects of equibiaxial in-plane tensile stresses on the ferroelectric and piezoelectric responses of tetragonal $BaTiO_3$. Although $BaTiO_3$ has a rhombohedral ground state at low temperature, tetragonal phase can be stabilized by controlling temperature or pressure and has been successively synthesized. It is expected that a theoretical study on $BaTiO_3$ under biaxial stresses is helpful for further understanding the electromechanical responses of relaxor ferroelectric single crystals and ferroelectric superlattices.

In this paper, we study the effects of equibiaxial tensile stresses on ferroelectricity and piezoelectricity of tetragonal $BaTiO_3$ using total energy as well as linear response calculations. We first find an anomalous phase transition to the paraelectric structure induced by stress. We also show the great enhancement of piezoelectricity near the phase-transition region. To reveal the underlying mechanism of ferroelectricity and piezoelectricity, we calculate the atomic displacements and the Born effective charges as a function of stress.

* Corresponding author.
E-mail addresses: yifeng@semi.ac.cn (Y. Duan), gangtang@cumt.edu.cn (G. Tang).

0925-8388/$ – see front matter © 2010 Elsevier B.V. All rights reserved.
doi:10.1016/j.jallcom.2010.08.005

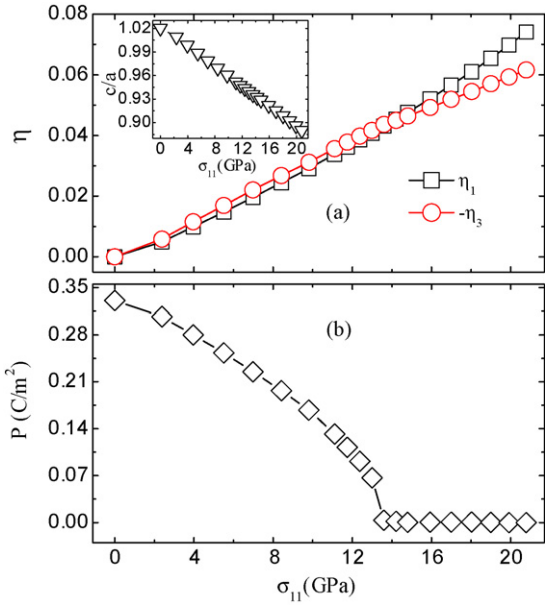

Fig. 1. In-plane tensile stress dependence of (a) strains η_1 and η_3, and (b) polarization P (C/m^2). The inset of panel (a) shows the c/a axial ratio with stress.

2. Computational methods

Our calculations are performed within the local density approximation (LDA) to the density functional theory (DFT) as implemented in the plane-wave pseudopotential ABINIT package [14–16]. To ensure good numerical convergence, the plane-wave energy cutoff is set to be 100 Ryd and a $6\times6\times6$ k-meshpoints are used. The norm-conserving pseudopotentials generated by the OPIUM program have been tested against the all-electron full-potential linearized augmented plane-wave method [17,18]. The orbitals of Ba $5s^25p^66s^2$, Ti $3s^23p^63d^24s^2$ and O $2s^22p^4$ are explicitly included as valence electrons. The dynamical matrices, atomic displacements in response to stess, and the Born effective charges are computed by the linear response theory of strain-type perturbations [19], and the electric polarization is calculated by the Berry-phase approach [20]. The piezoelectric strain coefficients $d_{iv} = \sum_{\mu=1}^{6} e_{i\mu}s_{\mu v}$, where e is the piezoelectric stress tensor and the elastic compliance tensor s is the reciprocal of the elastic stiffness tensor c (Roman indexes from 1 to 3, and Greek ones from 1 to 6).

To find the equilibrium lattice constants under zero pressure, we relaxed both the atomic positions and the primitive cell lattices until the largest stress tensor components (σ_{ij}) is less than 0.05 GPa. To reach the target equibiaxial tensile stress, we first apply a small equibiaxial tensile strain increment in the plane perpendicular to the c axis and conduct the full structural optimization for the lattice vector along the c axis and all the internal atomic positions until the stress σ_{33} is smaller than 0.05 GPa and $\sigma_{ij}=0$ for $i\neq j$. The strain is then increased step by step. The strains η_i are calculated using $\eta_1=\eta_2=(a-a_0)/a_0$ and $\eta_3=(c-c_0)/c_0$, where a_0 and c_0 are the LDA results of lattice constants of 3.915 and 3.995 Å, respectively, which are slightly less than the corresponding experimental values of 3.994 and 4.034 Å, respectively [21]. The agreement is typical of LDA calculation for ferroelectric perovskites [22], and the experimental volume corresponds to a negative hydrostatic pressure $P_0=-9.027$ GPa.

3. Results and discussion

Fig. 1 shows the strains η_1 and η_3, c/a axial ratio, and electric polarization along the c axis as a function of equibiaxial in-plane tensile stress σ_{11}. When the stress is below a critical value of about 13 GPa, the magnitude of η_3 is slightly larger than that of η_1, whereas the opposite is true as the stress further increases above the critical value. Meanwhile, accompanied with the nonlinear increases of η_1 and η_3, the c/a axial ratio decreases linearly with increasing σ_{11}. Fig. 1 also indicates the electric polarization as a function of stress σ_{11}. Under zero stress, the calculated polarization is 0.33 C/m^2, slightly larger than the theoretical value of 0.28 C/m^2 calculated at the experimental structure [8]. This is consistent with that the calculated lattice constant ratio c/a of 1.0204 is larger than that of 1.0098 for the experimental structure. As the stress increases, the polarization always decreases until reaching zero at the critical stress of about 13 GPa, suggesting the suppression of the ferroelectric instability and the ultimate transition to the paraelectric phase, similar to the case of hydrostatic pressure [23].

To further confirm the phase transition to the paraelectric structure, Fig. 2 is plotted to show the valence charge density in the (2 0 0) plane at equilibrium, maximum piezoelectricity and maximum stress studied, respectively. Following the evolution of charge density, we find that the orbital hybridization between Ti 3d and O_1 2p states becomes much and much weaker with increasing σ_{11}, consistent with the fact that the hybridization is sensitive to bond length [24]. Fig. 2 also shows that the charge density along the ⟨0 0 1⟩ direction becomes more and more symmetrical with increasing σ_{11}, suggesting the decrease in polarization and supporting the conclusion of phase transition.

Fig. 3 summarizes the stress effect on piezoelectricity. Under zero stress, the piezoelectric coefficients e_{33} and d_{33} are 4.79 C/m^2 and 35.61 pC/N, respectively. The piezoelectric coefficients are greatly enhanced by the appropriately applied epitaxial tensile stress near phase transition. The most significant enhancement is for e_{33} and d_{33} with the maximum values of 23.68 C/m^2 and 112.64 pC/N, respectively. Then all of these piezoelectric coefficients drop abruptly with further increasing stress and remain quite small for the paraelectric phase. In our present work, we only focus on the tetragonal $P4mm$ structure, the polarization always remains along the [0 0 1] direction before σ_{11} reaches the critical value, i.e., only the magnitude of polarization decreases with stress. Since the piezoelectric stress (strain) coefficients are the derivatives of the polarization with respect to the corresponding strain (stress), the peaks of piezoelectric response occur at the maximum slopes of the polarization versus stress curves near the phase-transition regions (see Fig. 1(b)). As a result, the predicted enhancement of electromechanical response originates from the change in the magnitude of polarization induced by stress. In Wu and Cohen's work [11], the predicted great enhancement of piezoelectric effect comes from

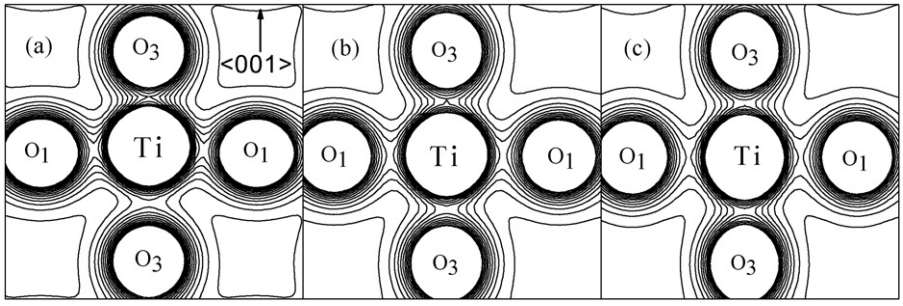

Fig. 2. Valence charge density in the (2 0 0) plane of tetragonal structure at equilibrium (a), maximum piezoelectricity (b) and maximum stress studied (c). The O_1 (O_2) atom is on the xz (yz) face of the primitive cell, and the O_3 atom is located between Ti atoms along the c axis.

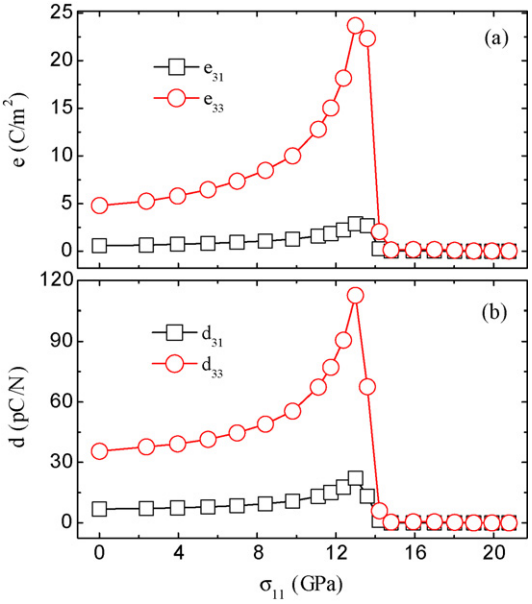

Fig. 3. In-plane tensile stress dependence of (a) piezoelectric stress coefficients e_{31} and e_{33} (C/m^2), and (b) piezoelectric strain coefficients d_{31} and d_{33} (pC/N).

noncollinear polarization rotation occurring at the phase-transition pressure.

To understand the underlying mechanisms responsible for the epitaxial-tensile-stress-induced behavior of polarization, we plot the atomic displacements μ_z, the Born effective charges Z^*, and the contributions of each atom to the total electric polarization as a function of stress, as displayed in Fig. 4. Since the atomic displacements and polarization in a tetragonal structure are all along the c axis, only Z^*_{zz} contribute to the polarization. As the stress increases, μ_z of Ba and Ti atoms always decrease from positive, while those of O atoms increase, until reaching their common value of −0.0336 Å for the paraelectric phase. That is to say that when the stress is above the critical value of about 13 GPa, if the Ba atom is set at (0, 0, 0), the Ti and O atoms are located at the body and face centers of the primitive cell, respectively, supporting the conclusion of phase transition. In contrast, Z^*_{zz} for all atoms barely change over the whole stress range studied. Z^*_{zz} of Ba and O_1 atoms are very close their normal charges, while those of Ti and O_3 are anomalously large, indicating the strong orbital hybridization between Ti and O_3 states, as shown in Fig. 2. Therefore, the epitaxial-stress-induced behavior of atomic displacements along the c axis leads to the change of magnitude of polarization, causing the predicted enhancement in piezoelectricity near phase transition.

Fig. 4(c) shows the contributions of each atom to the total electric polarization calculated by $P_i = Z^*_{zzi}\mu_{zi}/\Omega$, where Ω is the volume of the primitive cell studied, and Z^*_{zzi} and μ_{zi} are the Born effective charge and displacement of ion i in this cell, respectively, which satisfies $P = P_{Ba} + P_{Ti} + 2P_{O1} + P_{O3}$. P_{Ba}, P_{Ti}, P_{O1} and P_{O3} show the same trends as the total polarization, i.e., when σ_{11} increases, they decrease and finally remain constant for the paraelectric phase, consistent with the common paraelectric value of displacements for all atoms. The changes of P_{Ti} and P_{O3} are more obvious than those of P_{Ba} and P_{O1}, corresponding to the abnormally large Born effective charges Z^*_{zz} for Ti and O_3 atoms.

To further understand the relation between stress and strain (see Fig. 1(a)), Fig. 5 is plotted to show the elastic constants, bulk modulus B, and Young's modulus E along the a axis as a function of stress. The constants c_{12}, c_{13}, c_{44} and c_{66} almost remain constant and are much less than c_{11} and c_{33}. As σ_{11} increases, c_{11} always decreases, indicating that this material becomes soft along the non-

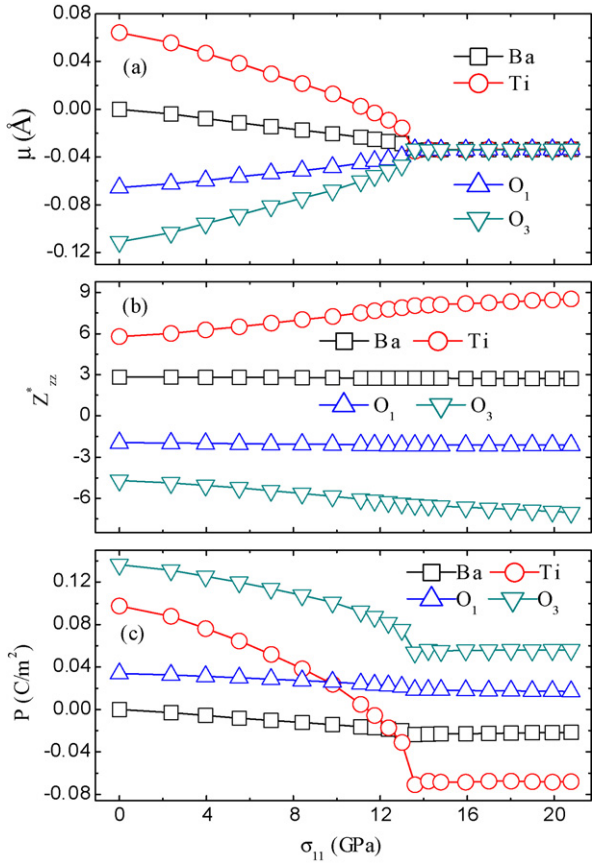

Fig. 4. In-plane tensile stress dependence of (a) the atomic displacements μ along the c axis (in Å) of the optimized structure relative to the centrosymmetric reference structure, (b) the Born effective charges Z^*_{zz}, and (c) the contributions of Ba, Ti, O_1 and O_3 atoms to the total polarization.

polar axes, whereas c_{33} dramatically increases, especially near the phase-transition stress, jumping from 247 to 373 GPa, suggesting that this material becomes markedly hard along the polar axis. We also summarize the effect of epitaxial stress on the bulk modulus B and Young's modulus E along the a axis, calculated by the elastic

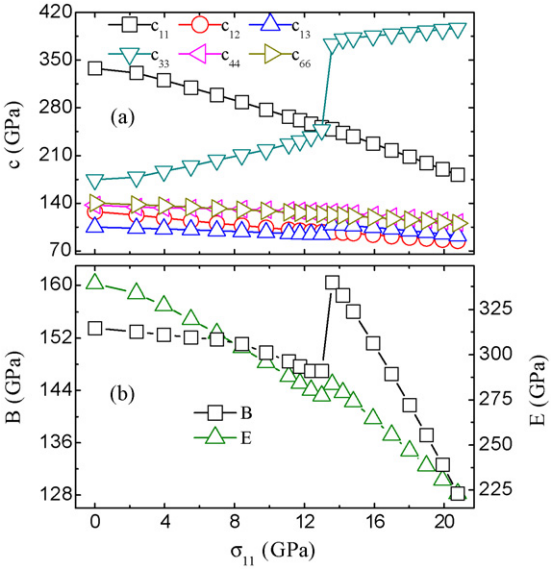

Fig. 5. In-plane tensile stress dependence of (a) elastic constants c_{ij} (GPa), and (b) bulk modulus B (GPa) and Young's modulus E along the a axis (GPa).

constants [25].

$$B_0 = \frac{(c_{11} + c_{12})c_{33} - 2c_{13}^2}{c_{11} + c_{12} + 2c_{33} - 4c_{13}} \quad (1)$$

$$E = c_{11} + c_{12} - \frac{2c_{13}^2}{c_{33}} \quad (2)$$

When the stress increases, B and E first decrease nonlinearly and jump to higher values at phase transition, and then decrease almost linearly, which emphasizes the conclusion of phase transition.

4. Summary

In summary, we have studied epitaxial tensile stress effects on ferroelectricity and piezoelectricity of tetragonal $BaTiO_3$ from first principles computations. We find anomalous phase transition and the enhancement of piezoelectricity occurring near the phase-transition region. The predicted enhancement of electromechanical response originates from the change in the magnitude of polarization, which is mainly attributed to the atomic displacements along the c axis, while the Born effective charges do not change significantly with stress. The trends of elastic constants, bulk modulus and Young's modulus along the a axis support the conclusion of phase transition. Our work suggests a way of enhancing the piezoelectric response, which would be helpful to enhance the performance of the piezoelectric devices.

Acknowledgments

The work is supported by the National Natural Science Foundation of China under Grant No. 10947119 and the Youth Science Funds of China University of Mining and Technology under Grant Nos. 2009A040 and 2009A048.

References

[1] K. Uchino, Piezoelectric Actuators and Ultrasonic Motors, Kluwer-Academic, Dordrecht, 1996.
[2] S.E. Park, T.R. Shrout, J. Appl. Phys. 82 (1997) 1804.
[3] R.F. Service, Science 275 (1997) 1878.
[4] Q. Wan, C. Chen, Y.P. Shen, J. Appl. Phys. 98 (2005) 024103.
[5] S.K. Jo, J.S. Park, Y.H. Han, J. Alloys Compd. 501 (2010) 259.
[6] G.-P. Du, Z.-J. Hu, Q.-F. Han, X.-M. Qin, W.-Z. Shi, J. Alloys Compd. 492 (2010) L79.
[7] Z.Ž. Lazarević, M.M. Vijatović, B.D. Stojanović, M.J. Romčević, N.Ž. Romcević, J. Alloys Compd. 494 (2010) 472.
[8] Y. Duan, H. Shi, L. Qin, J. Phys.: Condens. Matter 20 (2008) 175210.
[9] Y. Duan, J. Li, S.-S. Li, J.-B. Xia, C. Chen, J. Appl. Phys. 103 (2008) 083713.
[10] Y. Duan, L. Qin, G. Tang, C. Chen, J. Appl. Phys. 105 (2009) 033706.
[11] Z. Wu, R.E. Cohen, Phys. Rev. Lett. 95 (2005) 037601.
[12] Y. Duan, C. Wang, G. Tang, C. Chen, Nanoscale Res. Lett. 5 (2010) 448.
[13] Y. Duan, L. Qin, G. Tang, C. Chen, Phys. Lett. A 374 (2010) 2075.
[14] X. Gonze, J.M. Beuken, R. Caracas, F. Detraux, M. Fuchs, G. Rignanese, L. Sindic, M. Verstraete, G. Zerah, F. Jollet, M. Torrent, A. Roy, M. Mikami, Ph. Ghosez, J.Y. Raty, D.C. Allan, Comput. Mater. Sci. 25 (2002) 478.
[15] D.R. Hamann, X. Wu, K.M. Rabe, D. Vanderbilt, Phys. Rev. B 71 (2005) 035117.
[16] X. Wu, D. Vanderbilt, D.R. Hamann, Phys. Rev. B 72 (2005) 035105.
[17] A.M. Rappe, K.M. Rabe, E. Kaxiras, J.D. Joannopoulos, Phys. Rev. B 41 (1990) 1227.
[18] D.J. Singh, Planewaves, Pseudopotential, and the LAPW Method, Kluwer-Academic, Dordrecht, 1994.
[19] X. Gonze, C. Lee, Phys. Rev. B 55 (1997) 10355.
[20] R.D. King-Smith, D. Vanderbilt, Phys. Rev. B 47 (1993) 1651.
[21] H.T. Evans Jr., Acta Crystallogr. 14 (1961) 1019.
[22] Z. Wu, R.E. Cohen, D.J. Singh, Phys. Rev. B 70 (2004) 104112.
[23] I.A. Kornev, L. Bellaiche, P. Bouvier, P.E. Janolin, B. Dkhil, J. Kreisel, Phys. Rev. Lett. 95 (2005) 196804.
[24] W.A. Harrison, Electronic Structure and the Properties of Solids, Freeman, San Francisco, 1980.
[25] J.-M. Wagner, F. Bechstedt, Phys. Rev. B 66 (2002) 115202.